

Targeted alterations in iron homeostasis underlie plant defense responses

Guosheng Liu^{1,*}, David L. Greenshields^{1,*}, Ramaswami Sammynaiken², Rozina N. Hirji³, Gopalan Selvaraj³ and Yangdou Wei^{1,‡}

¹Department of Biology, University of Saskatchewan, 112 Science Place, Saskatoon, SK S7N 5E2, Canada

²Saskatchewan Structural Sciences Center, University of Saskatchewan, 110 Science Place, Saskatoon, SK S7N 5C9, Canada

³Plant Biotechnology Institute, National Research Council of Canada, 110 Gymnasium Place, Saskatoon, SK S7N 0W9, Canada

*These authors contributed equally to this work

‡Author for correspondence (e-mail: yangdou.wei@usask.ca)

Accepted 26 November 2006

J. Cell Sci. 120, 596-605 Published by The Company of Biologists 2007
doi:10.1242/jcs.001362

Summary

Iron (Fe) is a ubiquitous redox-active element essential for most life. The formation of localized cell wall appositions, the oxidative burst and the production of pathogenesis-related proteins are hallmarks of plant defense responses. Here, we report that iron is a central mediator linking these three phenomena. We show that in response to pathogen attack, reactive Fe³⁺, but not Fe²⁺, is deposited at cell wall appositions where it accumulates and mediates the oxidative burst. We provide evidence that the bulk secretion of Fe³⁺ provoked by pathogen attack leads to intracellular iron depletion, and that H₂O₂ itself induces ATP-dependent intracellular iron efflux. Finally, we demonstrate that this intracellular iron depletion promotes

the transcription of pathogenesis-related genes in concert with H₂O₂. This work identifies iron as an underlying factor associated with the oxidative burst and regulating cereal defenses, and establishes links between disease-related iron homeostasis in plants and animals.

Supplementary material available online at
<http://jcs.biologists.org/cgi/content/full/120/4/596/DC1>

Key words: Iron homeostasis, Reactive oxygen species, Plant defense, Cell wall apposition, Wheat powdery mildew, Prussian Blue staining

Introduction

Plants have evolved a series of coordinated defense responses rendering them inaccessible to most would-be pathogens. Despite diverse and specialized adaptive responses, plants also display some common innate or basal defenses against pathogens, including the formation of localized cell wall appositions (CWAs), a burst of reactive oxygen species (ROS) and production of pathogenesis-related (PR) proteins (Hückelhoven and Kogel, 2003; Schulze-Lefert, 2004). Many of the mechanisms underlying these defenses remain unresolved. CWAs are barriers commonly containing callose, cross-linked phenolics and proteins, and are an evolutionarily ancient but efficient means for host and nonhost plants to defend against microbial attacks (Schulze-Lefert, 2004). Recessive mutations in the barley *Mlo* gene confer durable, broad-spectrum resistance to powdery mildew pathogens through the production of oversized CWAs (Buschges et al., 1997). The *Arabidopsis pen1*, *pen2* and *pen3* mutants show a loss of penetration resistance to nonhost *Blumeria graminis* f. sp. *hordei* because of mutations in plasma membrane syntaxin, peroxisomal glycosyl hydrolase and ATP-binding cassette transporter genes, respectively (Assaad et al., 2004; Collins et al., 2003; Lipka et al., 2005; Stein et al., 2006). However, the precise roles of individual CWA components remain complicated; *Arabidopsis pmr4* plants, for example, which lack pathogen-induced callose deposition at CWAs, are more resistant to powdery mildew than wild-type plants (Nishimura et al., 2003). The establishment of CWAs is associated with

elevated levels of ROS at the site of infection (Thordal-Christensen et al., 1997; Wei et al., 1998). A variety of ROS-producing enzymes have been suggested to participate in creating the oxidative burst (Bolwell et al., 2002; Hückelhoven and Kogel, 2003; Torres et al., 2002), but no single enzyme system can conclusively account for ROS production across the continuum of plant-microbe interactions. Beyond roles in fortifying CWAs and toxicity to the pathogen, mounting evidence suggests that ROS also regulate several signaling pathways in plants (Mittler et al., 2004), including local and systemic signaling essential for plant innate immunity (Alvarez et al., 1998; Levine et al., 1994).

Iron (Fe) is essential for most life, but it also readily engages in one-electron reduction-oxidation (redox) reactions between its ferric (3⁺) and ferrous (2⁺) states that can catalyze the generation of toxic free radicals through the Fenton reaction (Pierre and Fontecave, 1999). In mammals, well-controlled Fe homeostasis is needed to prevent the Fe overload- and deficiency-related diseases hemochromatosis and anemia (Hentze et al., 2004). Similarly, to battle infection, macrophages need enough Fe to kill pathogens through the respiratory burst, but must keep Fe levels low enough to discourage pathogen growth (Alford et al., 1991; Schaible and Kaufmann, 2004). The fungal pathogen of humans, *Aspergillus fumigatus*, requires the ability to strip Fe from its host using low molecular weight siderophores in order to cause infection (Hissen et al., 2005; Schrettl et al., 2004). A role for Fe has also been reported in some plant diseases such as soft rot and

fire blight incited by the bacteria *Erwinia chrysanthemi* and *E. amylovora*, respectively (Expert, 1999), with a focus on Fe acquisition by pathogen. *Arabidopsis* ferritin withholds Fe from *E. chrysanthemi*, suggesting that ferritin is required for aspects of basal defence in that pathosystem (Dellagi et al., 2005). Correspondingly, in tobacco, ectopic expression of alfalfa ferritin enhances tolerance to ROS and the necrosis caused by viral and fungal infections (Deák et al., 1999).

We had previously noted a surprisingly high percentage of Fe-related transcripts in an expressed sequence tag (EST) library developed from wheat epidermis challenged with the wheat powdery mildew *Blumeria graminis* f. sp. *tritici* (*Bgt*), an important fungal pathogen worldwide (Liu et al., 2005). Together with reports of the importance of Fe in animal diseases (Alford et al., 1991; Hentze et al., 2004; Hissen et al., 2005; Schaible and Kaufmann, 2004; Schrettl et al., 2004; Smith et al., 1997), our EST data prompted us to investigate changes in Fe homeostasis in wheat leaves during *Bgt* attack.

Results

Fe³⁺ accumulates at pathogen attack sites

To characterize Fe homeostasis in pathogen-challenged plants at the tissue level, we used inductively coupled plasma mass spectrometry (ICPMS) to track any concentration changes in metals in the epidermis and mesophyll of wheat leaves inoculated with *Bgt*. To negate the effect of the spore iron content in the ICPMS readings, the leaves were wiped with moistened cotton and the removal of spores was confirmed by microscopic examination. We found that Fe accumulated in the infected epidermis 24 hours post-inoculation (hpi) (Fig. 1A), a time-point where CWAs are mature and the success or failure of the attempted infection is distinguishable. In contrast to the epidermis, the mesophyll did not show any significant changes in Fe content. Since we had seen a 55% increase in the Fe content of wheat epidermis following inoculation with *Bgt* (Fig. 1A), we wanted to determine where the Fe was accumulating at the cellular level. To localize Fe at the cellular level in *Bgt*-attacked wheat leaves, we adapted the Prussian Blue staining technique, previously used to study Fe accumulation in Alzheimer's disease (Smith et al., 1997), for use in our wheat-*Bgt* pathosystem. Plant Fe²⁺ staining was only found in the nuclei of the epidermal cells and in the fungal tissues (Fig. 1B). The Fe²⁺ staining of the fungal spores and germ tubes is consistent with a previous observation that ferric reductase activity is high in the spores and germ tubes of *B. graminis* f. sp. *hordei* (Wilson et al., 2003). In contrast to reduced Fe²⁺, oxidized Fe³⁺ staining was intense at the CWAs and at the edges of halo areas (Fig. 1C). Inoculated epidermal guard cells and trichomes also showed Fe³⁺ staining, but no staining occurred in uninoculated leaves (data not shown), implicating pathogen-responsive Fe accumulation in these structures as well. Fe³⁺ was found in the nuclei of epidermal cells with and without inoculation. We also found similar Fe³⁺ accumulation at CWAs in the other monocot crop plants barley, corn, millet, oat and sorghum (Fig. 1D), suggesting that the phenomenon is conserved throughout monocot plants. Together, these results show that in pathogen-attacked monocot leaves, Fe³⁺ is targeted to the epidermis where it accumulates in and around CWAs.

Pathogen attack causes a rapid remodeling of the host cell cytoskeleton and active streaming of cytoplasm towards sites

of contact in different pathosystems (Kobayashi et al., 1997; Koh et al., 2005; Škalamera and Heath, 1998; Takemoto et al., 2003). Endoplasmic reticulum, peroxisomes and Golgi bodies aggregate and accumulate at the infection site, suggesting that production and secretion of cellular components including secondary metabolites and proteins are activated around the penetration site (Koh et al., 2005; Takemoto et al., 2003). Actin filaments play a role in trafficking of vesicles and multivesicular endosomes in plant cells (An et al., 2006). To track the path of Fe to the infection sites and to investigate the role of actin in this process, we treated freshly inoculated leaves with the actin filament disruptor cytochalasin A (cytA). In leaves treated with 1 µg ml⁻¹ cytA, Fe³⁺ was present at 55% fewer appressorial germ tube-associated CWAs than in water-treated control leaves (Fig. 1E), suggesting that actin guides vesicle-like bodies destined for CWAs. Whereas the majority of Fe-positive sites following cytA treatment showed only weak Fe accumulation centrally in the CWA, Fe accumulation at the outer CWA haloes was completely abolished (compare Fig. 1C with Fig. 1E). CytA also blocked cytoplasmic aggregation and nuclear migration subjacent to sites of attack (Fig. 1E). We also investigated the role of microtubules in iron accumulation at CWAs by treating inoculated leaves with the microtubule-depolymerizing agent oryzalin (Mathur and Chua, 2000), but found no difference between oryzalin-treated and untreated leaves (data not shown). Together, these results show that in wheat leaves, cytosolic Fe³⁺ is transported to CWAs in vesicle-like bodies guided by actin polymerization.

The Fe³⁺ at CWAs is chelatable and redox-active

To examine whether the stained Fe³⁺ in CWAs was firmly bound to proteins, we treated infected epidermal tissues with 10 mM deferoxamine (DFO) prior to staining. DFO is a Fe³⁺-specific high-affinity bacterial siderophore with a stability constant for Fe³⁺ of 10³¹, but does not remove Fe from heme proteins (Keyer and Imlay, 1996) (supplementary material Fig. S1). Fe³⁺ staining in CWAs was completely abolished by DFO treatment, although the CWAs and associated cytoplasmic aggregations were still apparent beneath the fungal penetration attempts (Fig. 2A). By contrast, DFO treatment did not eliminate Fe³⁺ staining in fungal tissues.

To ensure that the observed chelatable Fe accumulation in and around CWAs was not an artifact of our fixation and staining methods, we used the membrane-impermeable Fe³⁺-binding fluorescent dye calcein to examine Fe accumulation in fresh leaf samples. Calcein has a stability constant for Fe³⁺ of 10²⁴, which is lower than the stability of EDTA-Fe³⁺, but higher than that of citrate-Fe³⁺. Binding of Fe³⁺ to calcein quenches its fluorescence, providing a reliable indicator of labile Fe in biological systems (Thomas et al., 1999). Fig. 2B (left panel) shows that prior to treatment with DFO, calcein fluorescence is quenched in the CWAs of wheat leaves 24 hpi, indicating the presence of labile or reactive Fe in these structures. Following DFO treatment, however, there was enhanced calcein fluorescence at CWAs, indicative of Fe removal, whereas the Fe within the fungal structures remained unchanged (Fig. 2B, right panel).

To further investigate the oxidation states and lability of the accumulating Fe in pathogen-challenged wheat leaves, we compared intact leaves before and 24 hpi with *Bgt* using electron paramagnetic resonance (EPR) spectroscopy. The

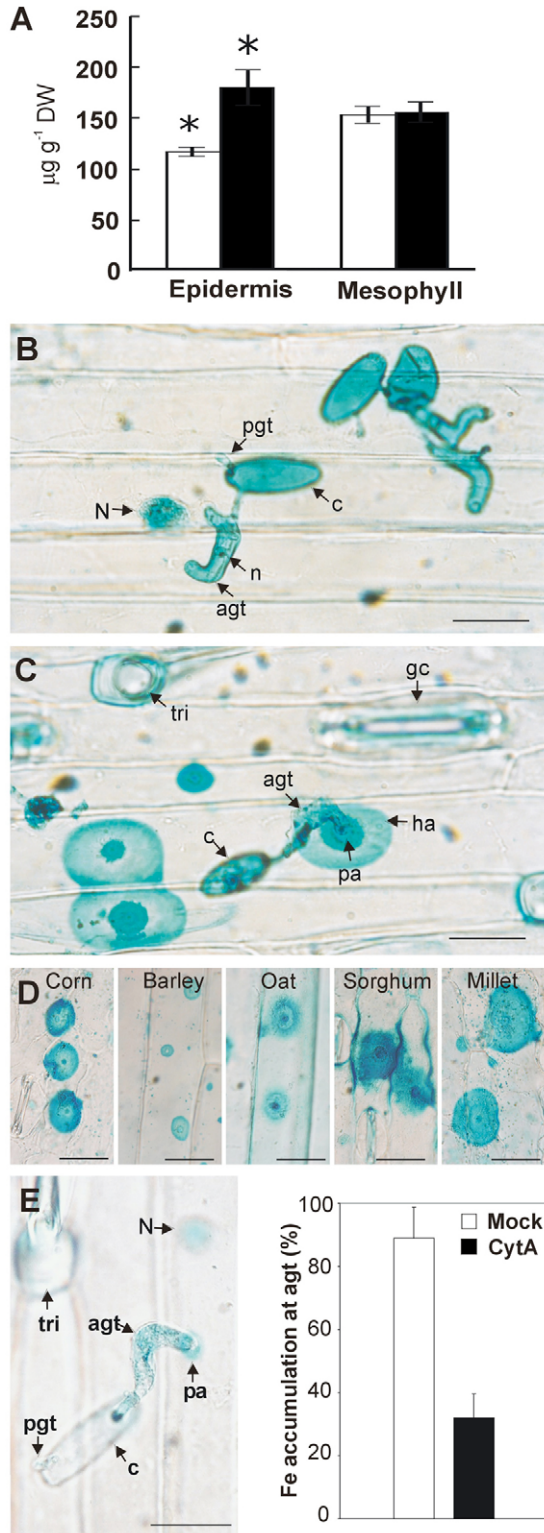


Fig. 1. Targeted Fe redistribution in wheat leaves after *Bgt* attack. (A) Fe concentration increases in *Bgt*-attacked tissue. Metal concentrations determined by ICPMS analysis of wheat leaf epidermal cells and underlying mesophyll cells in response to *Bgt* attack, 24 hpi (filled bars) or before inoculation (open bars). The mean values (\pm s.d.) of three independent treatments are shown. Asterisks indicate significant difference ($P < 0.01$) before and after inoculation, based on Student's *t*-test. (B) In situ Fe^{2+} Prussian Blue staining of wheat epidermis 24 hpi with *Bgt*. (C) In situ Fe^{3+} Prussian Blue staining of wheat epidermis 24 hpi with *Bgt*. (D) In situ Fe^{3+} Prussian Blue staining of epidermal peels 24 hpi with *Bgt* in corn, barley, oat, sorghum and millet. (E) The actin filament disruptor cytochalasin A (cytA) blocks Fe accumulation at CWAs. Graph shows the reduction in Fe^{3+} accumulation at agt-associated CWAs (means \pm s.d., $n=300$ based on 100 *Bgt* attack sites per leaf on three leaves). agt, appressorial germ tube; c, conidium; ha, halo; gc, guard cell; N, epidermal nucleus; n, fungal nucleus; pa, papilla; pgt, primary germ tube; tri, trichome. Scale bar, 20 μm .

with a single isotropic feature at $g=2.0$ was also observed in both control and inoculated leaves, and yielded a more intense spectrum in inoculated leaves. High-resolution scanning using variable temperatures revealed a broad feature of the mixture of low-spin Fe^{3+} with free radicals (Fig. 2C, right inset) (Clay et al., 2002). The dramatic increase in EPR-detectable Fe^{3+} following infection could reflect either the increased transport of Fe^{3+} into infected leaves, the oxidation of the Fe pool in infected leaves, or a combination of both of these. These results demonstrate that in response to *Bgt* attack, Fe^{3+} is deposited and accumulates at CWAs in a redox-active form.

Accumulated Fe mediates the oxidative burst at CWAs

CWAs are the site of an intense, localized burst of ROS that is thought to fortify the CWAs, physically damage the pathogen and regulate downstream resistance signaling events. It has been suggested that 3,3'-diaminobenzidine (DAB) staining can specifically localize H_2O_2 in planta (Thordal-Christensen et al., 1997). To investigate the chemistry behind DAB staining, we performed in vitro assays using combinations of peroxidase, H_2O_2 , Fe^{3+} and DFO (see supplementary material Fig. S1). Although neither H_2O_2 , Fe^{3+} nor peroxidase alone could oxidize DAB, H_2O_2 could oxidize DAB to produce the color reaction in the presence of either Fe^{3+} or peroxidase. These reactions suggest that the ability of DAB to localize H_2O_2 is hinged on the presence of an intermediate able to transfer electrons from DAB to H_2O_2 . We found the strong reddish-brown color of oxidized DAB in wheat leaf epidermis in response to *Bgt* in and around CWAs subjacent to the primary and appressorial germ tubes (Fig. 3A). In animal macrophages, the respiratory burst is dependent on Fe (Schaible and Kaufmann, 2004). Because the reactive Fe that accumulated in CWAs could participate in the generation of H_2O_2 as it does in mammalian cells (Hentze et al., 2004; Smith et al., 1997), we double stained *Bgt*-inoculated wheat leaves for H_2O_2 and Fe^{3+} using DAB followed by Prussian Blue at different time points after inoculation to investigate a possible relationship. DAB staining was more pronounced centrally in CWAs and the inner layer of the haloes, whereas Prussian Blue staining was more intense along the edges of haloes surrounding the yellow-brown DAB (Fig. 3B). This same staining pattern was also observed at primary germ tube-associated CWAs as early as 4 hpi (Fig. 3C). Vesicle-like bodies double stained for Fe^{3+} and

EPR spectra of control and inoculated leaves are shown in Fig. 2C. The intensity of the Fe^{3+} signal at $g=4.3$, 5.0 and 5.8, which represents a high-spin state Fe^{3+} as would be expected for a weakly bound system, was 4–5 times higher in leaves 24 hpi than in control leaves (Fig. 2C, left inset), indicating an increase in redox-active Fe after *Bgt* attack. A strong signal

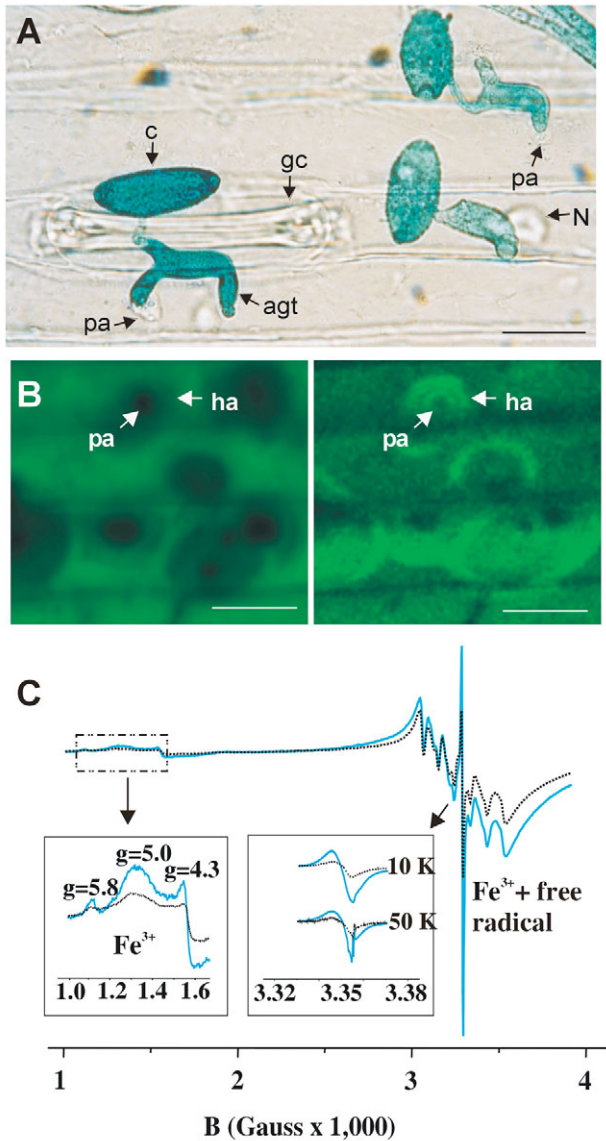


Fig. 2. Chelatable, redox-active Fe accumulation in wheat leaves after *Bgt* attack. (A) Wheat epidermis 24 hpi with *Bgt* stained for Fe^{3+} after pretreatment with the Fe^{3+} chelator DFO. (B) In situ calcein staining of Fe^{3+} in wheat leaves 24 hpi with *Bgt* before (left panel) and after (right panel) treatment with the Fe chelator DFO. (C) Wide-range X-band EPR spectrometry of wheat leaves 24 hpi with (blue solid line) or without (black broken line) *Bgt* inoculation. Insets are the enlarged high-resolution scanning for high-spin and low-spin Fe^{3+} , respectively. The g values of high-spin Fe^{3+} are indicated. Spectral intensities were normalized relative to sample amount. Two independent experiments showed similar results. agt, appressorial germ tube; c, conidium; ha, halo; gc, guard cell; N, epidermal nucleus; pa, papilla. Scale bar, 20 μm .

H_2O_2 were also found centrally in CWAs (Fig. 3D). These vesicle-like bodies are interesting considering the effect of cytA on CWA Fe deposition. They are made up of a mixture of small papillae and large multivesicular components, such as multivesicular bodies and paramural bodies (An et al., 2006), and have previously been shown to contain H_2O_2 in *B. graminis* f. sp. *hordei*-attacked barley cells (Collins et al., 2003; Hüchelhoven et al., 1999).

Although the double staining showed an association between Fe^{3+} and H_2O_2 , it did not allow us to decipher whether or not the accumulated redox-active Fe was involved in the oxidative burst. To determine whether the accumulated Fe mediates this DAB-detectable oxidative burst, we pretreated inoculated fresh wheat leaves with DFO for 6 hours prior to DAB staining, but found no difference in the macroscopic appearance of the DFO-treated and untreated leaves (Fig. 3E). Surprisingly, however, the DFO blocked DAB oxidation at CWAs, indicating that Fe, rather than peroxidase (Thordal-Christensen et al., 1997), is required specifically for DAB oxidation at pathogen attack sites (Fig. 3F,G). The inhibitory effect of DFO on DAB staining was concentration dependent. At concentrations below 2 mM, DFO had no effect on the ability of the fungus to penetrate the host epidermal cells but efficiently abolished the DAB staining (data not shown). At concentrations above 3 mM, however, the fungal spores produced smaller, misshapen appressorial germ tubes. Cytoplasmic aggregation and nuclear migration were still apparent beneath sites of *Bgt* attack following DFO treatment (Fig. 3G,H), suggesting that this DFO treatment chelated Fe without blocking other processes relevant to CWA formation. Taken together, these data show that the reactive Fe that accumulates at CWAs mediates the DAB-detectable oxidative burst during pathogen attack.

Fe regulates gene expression through redox-dependent and -independent pathways

We established a regime of Fe treatment that could mimic the accumulation of Fe and the accompanying apoplastic H_2O_2 production in wheat leaves (Fig. 4A,B), and used mRNA from leaves under this treatment to probe an array of 145 genes mined from a *Bgt*-infected wheat epidermis-derived EST library (see supplementary material Table S1). A similar approach has identified a range of Fe-regulatory networks in humans (Muckenthaler et al., 2003). Among the most Fe-inducible genes were members of the Fe homeostasis and *PR* gene functional groupings (Fig. 4C,D). The Fe homeostasis genes *TmNAS1* and *TmFER1*, encoding a nicotianamine (NA) synthase and ferritin isoform, respectively, were induced by Fe treatment in a concentration-dependent manner, regardless of the redox status of the leaves (Fig. 4E). The *PR* genes were induced only by Fe concentrations $>500 \mu\text{M}$ and this induction was blocked by addition of the redox buffer glutathione (GSH) (Fig. 4E). Together, these results suggest that Fe regulates gene expression through both Fe itself (i.e. the Fe homeostasis-related genes) and Fe-mediated oxidative stress (i.e. the *PR* genes).

Pathogen attack promotes cytosolic Fe depletion

Having established molecular probes to report the Fe content of wheat plants, we performed semi-quantitative reverse transcription-polymerase chain reaction (RT-PCR) analysis using primers specific for the representative Fe-homeostasis and *PR* genes with cDNA from either the epidermis or mesophyll of *Bgt*-inoculated wheat leaves. Surprisingly, expression of *TmFER1* and *TmNAS1* was downregulated 24 hpi (Fig. 5A), suggesting cytosolic Fe depletion in these tissues. The expression of *PR* genes was induced by infection as expected, probably due in part to the oxidative burst associated with the plant defense response. To understand whether the observed changes in gene expression were pathogenesis-related, we used *TmPR1b* and *TmNAS1* as representative genes

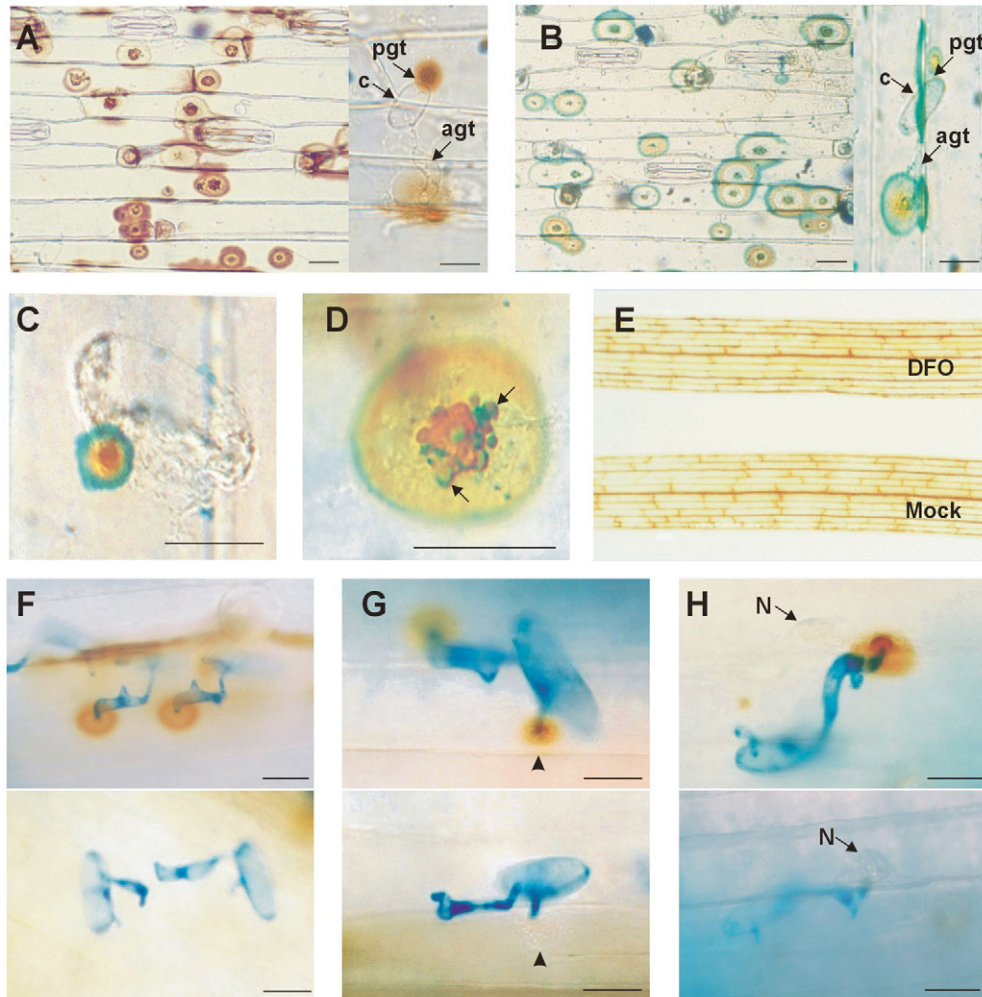


Fig. 3. Fe accumulation mediates DAB oxidation at CWAs. (A) H_2O_2 accumulation in CWAs revealed by DAB staining 24 hpi. (B) Double staining for H_2O_2 and Fe^{3+} (blue) 24 hpi. (C) Double staining for H_2O_2 and Fe^{3+} at a primary germ tube-associated CWA 5 hpi. (D) Vesicle-like bodies within a CWA double stained for H_2O_2 and Fe^{3+} 24 hpi. (E) Wheat leaves with (right) or without (left) pretreatment of 1.5 mM DFO were stained using DAB and photographed 24 hpi. (F–H) DFO blocks H_2O_2 generation at CWAs. Upper panel: without DFO pretreatment. Lower panel: with 1.5 mM DFO pretreatment. (F) DFO blocks H_2O_2 generation at appressorial germ tube-associated CWAs. (G) DFO blocks H_2O_2 generation at primary germ tube-associated CWAs but not cytoplasmic aggregation (arrowhead). (H) Pretreatment with DFO does not affect nuclear migration (arrows) at CWAs. agt, appressorial germ tube; c, conidium; N, host nucleus; pgt, primary germ tube. Scale bar, 20 μm .

and examined their expression over a 72-hour *Bgt* infection time course using northern analysis. Beginning at 6 hpi and ending at 48 hpi, a period linked to the formation of primary and appressorial germ tube-associated CWAs and apoplastic Fe accumulation, *TmNAS1* was downregulated whereas *PR1b* was upregulated (Fig. 5B), supporting the hypothesized Fe depletion in response to pathogen attack.

To further characterize the interplay between this possible cytosolic Fe depletion and H_2O_2 as regulators of gene expression, we tracked gene expression in plants treated with either DFO or DFO in combination with H_2O_2 . Depletion of cytosolic Fe by DFO abolished the *TmNAS1* and *TmFER1* expression as expected. The *PR* gene expression, however, was induced by both DFO and H_2O_2 , and in combination, DFO and H_2O_2 showed an additive promotion of *PR* gene expression (Fig. 5C). These data suggest that pathogen attack could promote cytosolic Fe depletion, and that *PR* gene expression is induced by cytosolic Fe depletion in concert with H_2O_2 .

H_2O_2 treatment causes cellular Fe efflux

We hypothesize that cytosolic Fe deficiency is provoked by powdery mildew attack. To understand whether apoplastic H_2O_2 generation is involved in this cytosolic Fe depletion, we adapted a wheat cell culture system combined with the fluorescent Fe indicator calcein-AM (nonfluorescent, membrane-permeable because of the conjugation of calcein with acetomethoxy ester, but once inside cells, they are hydrolyzed by nonspecific esterases, yielding fluorescent compound) and confocal microscopy to monitor cytosolic Fe concentrations during H_2O_2 treatment (Fig. 6A). Following cellular uptake of calcein-AM, intracellular esterases convert the molecule into a nonpermeable acid-form of calcein that binds Fe. Remarkably, treatment of calcein-AM-loaded cells with H_2O_2 led to a 5-fold increase in calcein fluorescence, indicating depletion of calcein-available Fe in the cells (Fig. 6B). The depletion of Fe following treatment of the cells with H_2O_2 could be interpreted in several ways including, but not

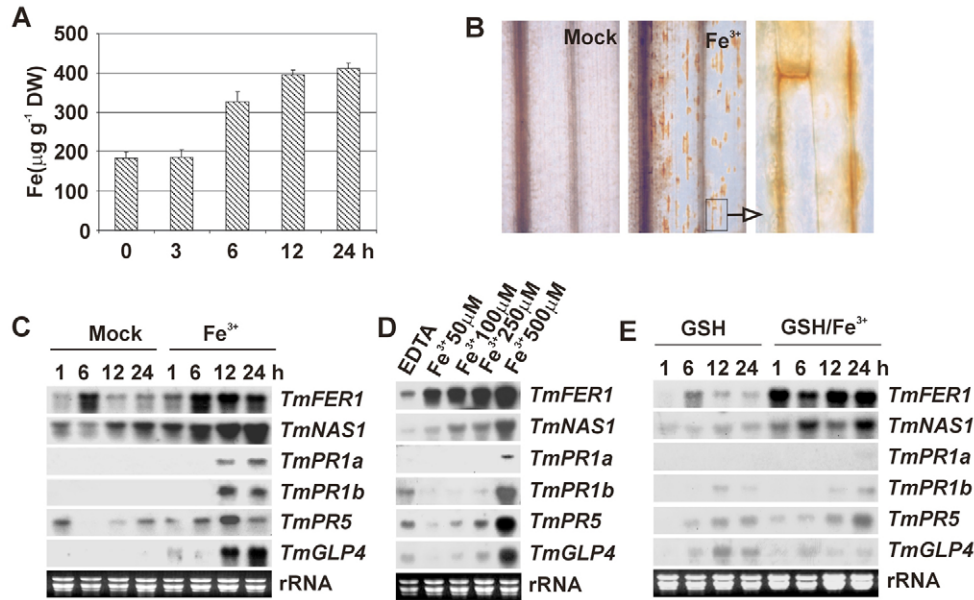


Fig. 4. Fe overload causes apoplastic H₂O₂ production and induces Fe homeostasis- and defense-related gene expression. (A) ICPMS analysis of Fe³⁺-EDTA uptake in wheat leaves. Values represent mean ± s.d. (*n*=3). (B) DAB staining for H₂O₂ in wheat leaves 12 hours after treatment with either Fe³⁺-EDTA (middle and right panels) or EDTA (Mock, left panel). (C) Northern blot analysis of time-dependent induction of Fe homeostasis- and defense-related genes following loading with 500 µM EDTA (Mock) or 500 µM Fe³⁺-EDTA at the time points indicated. Even loading of total RNA was monitored by ethidium bromide staining of rRNA. (D) Northern blot analysis of Fe³⁺-EDTA concentration-dependent gene expression. (E) Northern blot analysis of Fe³⁺-dependent and H₂O₂-dependent gene expression.

limited to, the complexation of cellular Fe with stronger chelators (phytosiderophores) activated or synthesized de novo; the sequestration of cellular Fe to organelles where calcein is stripped of Fe; or efflux of cellular Fe.

To further investigate H₂O₂-induced cytosolic Fe depletion, we treated the wheat suspension cells in media supplemented with either a glucose/glucose oxidase (G/GO) H₂O₂ generation system or H₂O₂ itself and then measured the Fe content of the culture supernatant using a spectrophotometric assay based on the absorbance of Ferrozine-bound Fe. As shown in Fig. 6C, Fe efflux is promoted by both the G/GO system and by H₂O₂ directly, leading to a 45% higher Fe concentration than in the supernatant of control cells. The G/GO H₂O₂ generation system can result in low but sustained accumulation of H₂O₂ in cell suspensions (Alvarez et al., 1998) and induced a similar amount of Fe efflux as 10 mM H₂O₂ (Fig. 6C). As expected, catalase was an efficient inhibitor of Fe efflux, confirming that Fe efflux is induced by H₂O₂. Interestingly, the ATPase inhibitor vanadate inhibited the H₂O₂-induced Fe efflux, regardless of the source of the H₂O₂, showing that this Fe efflux is an active process. The protein synthesis inhibitor cyclohexamide, however, did not appreciably inhibit the Fe efflux (Fig. 6D). Taken together, these data suggest that H₂O₂ promotes active cytosolic Fe efflux.

Discussion

Redistribution of Fe in response to pathogen attack

We had initially noted an enrichment of Fe- and redox-related transcripts in an EST collection of *Bgt*-infected *T. monococcum* epidermis (Liu et al., 2005). We have now shown localized and targeted redistribution of Fe in infected plant tissues and cells. Since unregulated changes in Fe concentrations can be dangerous (Hentze et al., 2004; Schaible and Kaufmann, 2004),

this strategy employed by plants appears to avoid deleterious effects while providing a function with respect to plant defense.

In animals, the best-studied route of Fe uptake is the endocytosis of Fe complexed with transferrin and the transferrin receptor, but nontransferrin-bound Fe can also be taken up directly through the divalent metal transporter DMT-1 (Hentze et al., 2004; Schaible and Kaufmann, 2004). DMT-1 is also responsible for efflux of Fe from the transferrin-Fe uptake endosomes into the cytosol, while cytosolic Fe is pumped out of the cell by the permease ferriportin. The loading of Fe into secretory vesicles following *Bgt* attack might require a transporter, as no known transferrin homologues exist in higher plants. Several types of Fe transporters have been identified in plants, including the natural resistance-associated macrophage protein, ZRT/IRT-like protein, ATP-binding cassette (ABC) and yellow stripe families (Hall and Williams, 2003), but this knowledge is largely restricted to aspects of developmental Fe acquisition and is complicated by the presence of multiple isoforms.

Vesicle-like bodies containing H₂O₂ can be observed moving towards the CWAs in challenged host cells (Collins et al., 2003; Hückelhoven et al., 1999). Similarly, we showed Fe-laden vesicle-like bodies in transit to and coalescing with CWAs. Recently, components of the SNARE complex have been identified as important mediators of CWA formation in barley and *Arabidopsis*, mediating exocytosis of CWA constituents to the apoplast (Assaad et al., 2004; Collins et al., 2003). Interestingly, in *Drosophila* an H⁺/ATPase was also found to be essential for a late step in synaptic vesicle exocytosis (Hiesinger et al., 2005), suggesting that Fe-efflux inhibition by vanadate might be related to vesicle secretion. PEN3, which contributes to nonhost penetration resistance, was found to encode an ABC-

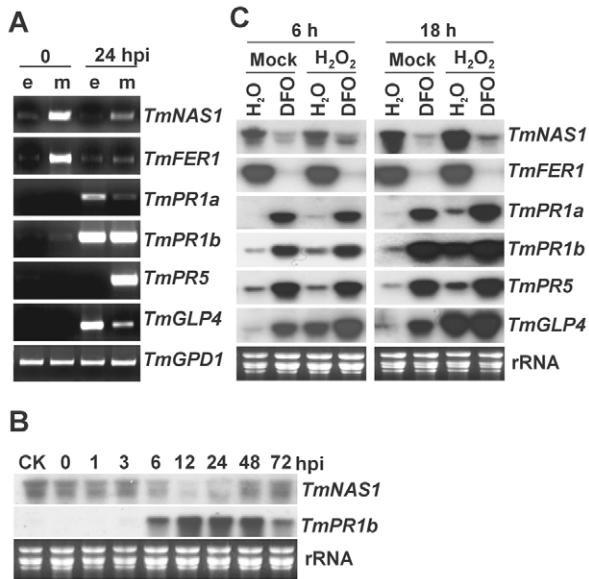


Fig. 5. Pathogen attack promotes cytosolic Fe depletion, leading to defense gene expression. (A) RT-PCR of mRNAs from epidermal (e) and mesophyll (m) tissues of wheat leaves before (0 hpi) and after (24 hpi) inoculation with *Bgt*. *TmGPD1* was used to check equal mRNA usage. (B) Northern blot analysis of *TmNAS1* and *TmPR1b* expression in wheat leaves 0–72 hpi with *Bgt*. (C) Northern blot analysis of total RNA from wheat leaves treated with either DFO alone or DFO followed by H_2O_2 for either 6 or 18 hours.

type transporter (Stein et al., 2006). A recent report also showed that Fe is pumped out of macrophages through an ABC-type transporter MPR1 (Watts et al., 2006). To be soluble and transportable in living cells, Fe must be chelated with natural ligands, which in plants include di- and tri-carboxylic acids, amino acids, amides, amines and especially NA (Curie and Briat, 2003; Ling et al., 1999). cDNA microarray analysis showed a correlation between the transcriptional regulation of NA synthesis and polar vesicle secretion (Negishi et al., 2002). The systemic acquired resistance (SAR) regulator NPR1, which is required for expression of *PR* genes, was also found to regulate the protein secretion pathway in *Arabidopsis*, revealing a link between these processes (Wang et al., 2005).

Apoplastic Fe and the oxidative burst

It is generally believed that generation of ROS promotes cross-linking of cell wall components leading to the development of CWAs, localized physical barriers to pathogen invasion (Schulze-Lefert, 2004; Thordal-Christensen et al., 1997). Beyond this, ROS production can take the form of so-called microbursts that perpetuate a signal leading to the development of SAR (Levine et al., 1994). In the model dicot plant *Arabidopsis*, superoxide (O_2^-) is produced by nicotinamide adenine dinucleotide phosphate (NADPH) oxidase during hypersensitive cell death (Torres et al., 2002). It was previously shown that the localized burst of H_2O_2 at barley CWAs is not sensitive to the NADPH oxidase inhibitor diphenyleneiodonium, and that superoxide is produced only in association with failed CWAs at successful penetration sites (Hückelhoven and Kogel, 2003). Like barley, the diploid wheat system used here is insensitive to diphenyleneiodonium (data not

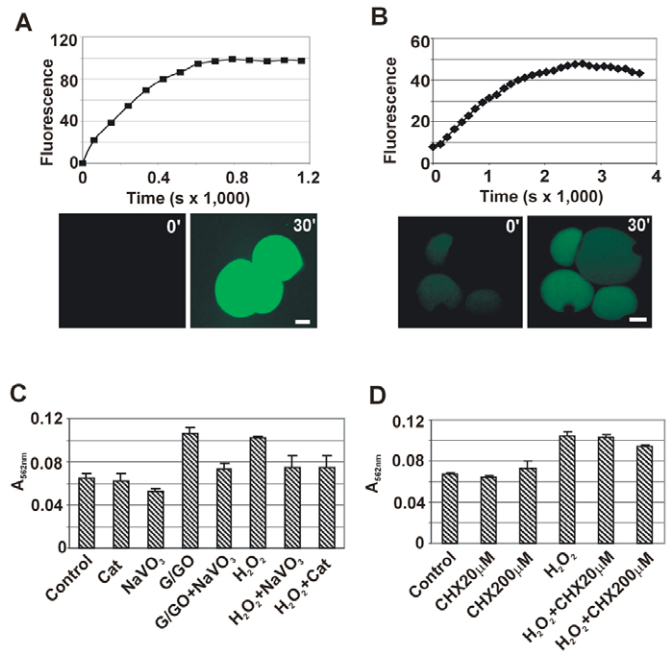


Fig. 6. H_2O_2 promotes cytosolic Fe depletion and Fe efflux. (A,B) Confocal imaging of Fe depletion in wheat suspension cells, based on calcein-AM fluorescence. Images (lower panels) depict the fluorescence at representative time points. Scale bar, 20 μ m. Time course of calcein-AM uptake (A); H_2O_2 -mediated cytosolic Fe depletion (B). (C,D) H_2O_2 -induced Fe efflux in wheat suspension cells. Bar values represent mean \pm s.d. ($n=3$). Cells were treated with glucose/glucose oxidase (G/GO) (5 mM/5 U ml $^{-1}$) or H_2O_2 (10 mM), with or without catalase (Cat) (10 U ml $^{-1}$) or vanadate ($NaVO_3$) (100 μ M), respectively (C); cells treated with 10 mM H_2O_2 and 20 or 200 μ M cycloheximide (CHX) (D).

shown). The difference between monocot and dicot pathogen-induced ROS generation systems is further supported by a lack of detectable Fe^{3+} at *Arabidopsis* CWAs (data not shown). In Alzheimer's disease-affected brains, Fe^{3+} is localized to lesions characteristic of the disease, where it participates in oxidative damage to the brain (Smith et al., 1997). We have now shown that the oxidative burst in cereals is reliant on Fe accumulation at CWAs, in a manner similar to that seen in Alzheimer's disease.

While in transit and after having been deposited to the apoplast, the Fe we observed was in a 'free' or 'chelatable' form, as it was EPR-detectable and readily removed by DFO. In mammalian cells, free Fe is recognized as a major cause of oxidative stress and toxicity in specific tissues and cell types (liver, macrophages and brain) (Hentze et al., 2004; Smith et al., 1997). Because of the overwhelming complexity of biological systems and the ability to analyze only limited aspects of a given system at one time, the role of transition metals in producing ROS in biological systems remains far from clear. The supposed role of Fe in ROS production is often summarized by the Fenton/Haber-Weiss reactions (Pierre and Fontecave, 1999) as follows:



Interestingly, only Fe^{3+} was found at CWAs, suggesting that

H_2O_2 is in excess and the Fe^{2+} is rapidly oxidized to Fe^{3+} at CWAs. However, this explanation seems to be at odds with the ability of DFO, a free Fe chelator, to prevent H_2O_2 production at CWAs by chelating the free Fe^{3+} . Supplementary material Fig. S1 shows that neither Fe^{3+} nor H_2O_2 alone are capable of oxidizing DAB in vitro, but in combination they produce the color reaction. This $\text{Fe}^{3+}/\text{H}_2\text{O}_2$ -dependent process is responsible for the majority of the in planta DAB reaction, as DFO was able to abolish the stain but had little effect on the peroxidase/ H_2O_2 -dependent DAB reaction. It also remains possible that the bulk of the H_2O_2 at CWAs is converted to OH^\cdot , and that the DAB is oxidized by OH^\cdot , rather than H_2O_2 , to produce the observed color reaction. This line of reasoning is supported by the EPR spectrum of inoculated wheat leaves, which showed a strong free radical peak mixed with low-spin Fe^{3+} . While DFO is unable to chelate Fe from Fe-containing peroxidase, studies have shown increases in peroxidase gene transcription (Liu et al., 2005) and peroxidase protein localization (Scott-Craig et al., 1995) in powdery mildew-challenged epidermal tissue. These induced peroxidases are probably producing H_2O_2 in challenged plants, suggesting either that the peroxidase activity alone is not enough to oxidize a visible amount of DAB, or that Fe is loaded into peroxidases at the cell wall, a process necessary for enzyme activity (Passardi et al., 2004), and that DFO blocks this Fe loading. Regardless of the chemistry by which it occurs, the blocking of CWA-associated H_2O_2 generation by DFO shows that Fe is essential for the oxidative burst. Much of the power of this hypothesized system of ROS generation lies in the rigid localization of Fe and H_2O_2 within CWAs. In contrast to leaves treated with excess Fe, where H_2O_2 production occurs broadly throughout the apoplast, in response to *Bgt* attack, H_2O_2 accumulation is highly focused to the points of attack.

Cytosolic Fe depletion and defense gene expression

Extensive work in animal systems has revealed a complex regulatory network for Fe homeostasis at the cellular and systemic levels (Hentze et al., 2004). Cellular Fe uptake and storage are coordinately controlled by binding of Fe-regulatory proteins IRP1 and IRP2 to Fe-responsive elements within the mRNAs [5'- or 3'-untranslated region (UTR)] encoding ferritin and the transferrin receptor, thus mediating regulation at post-transcriptional level. In plants, no such regulation system has yet been found and Fe-homeostasis genes appear to be both transcriptionally and post-transcriptionally controlled (Briat et al., 1999; Petit et al., 2001). Ferritin is a major Fe storage protein in plants as well as in animals, and can be used as a marker of cellular Fe content, although different isoforms behave differently in response to Fe conditions (Briat et al., 1999; Dellagi et al., 2005; Petit et al., 2001; Torti and Torti, 2002). In this study, we identified that *TmFER1* was specifically induced by Fe overload and suppressed by Fe depletion, proving it to be an excellent probe for monitoring intracellular Fe status. Unlike animals, however, plants also use the low molecular weight siderophore NA, which is probably involved in Fe long-distance transport (Curie and Briat, 2003) and in buffering free Fe in root and leaf cells (Pich et al., 2001). By using the Fe-sensitive gene *TmNAS1* along with *TmFER1*, we demonstrated that *Bgt*-attacked tissues are intracellularly Fe deficient.

Using wheat suspension cells and the membrane-permeable fluorescent chelator calcein-AM, we demonstrated the intracellular Fe depletion after treatment with H_2O_2 . In agreement with our

findings, a study in mammalian cells also reported that H_2O_2 treatment induced cytosolic Fe-deficiency exhibited by ferritin synthesis inhibition, transferring receptor synthesis induction and promotion of intracellular Fe redistribution in a time-dependent manner (Caltagirone et al., 2001). During pathogen infection, host-imposed metal ion limitation might be a strategy for immunity (Schaible and Kaufmann, 2004). We found that the Fe deficiency induced by *Bgt* attack is accompanied by the induction of *PR* genes, and that the induction is promoted by application of the Fe chelator DFO. The mechanism by which Fe deficiency regulates defense gene expression remains unresolved, but it is plausible that Fe homeostasis-mediated redox changes act as the trigger. In animals, Fe depletion regulates expression of a set of genes directly involved in Fe metabolism or interlinked pathways such as hypoxia, oxidative stress or nitric oxide metabolism (Hentze et al., 2004). Fe deficiency is also known to disrupt Fe-S cluster proteins (enzymes involved in redox or direct redox sensors), cause oxidative damage in mitochondria and trigger inflammatory-related genes (Walter et al., 2002; Choi et al., 2004). The sequestration of Fe by ferritin heavy chain suppresses ROS accumulation, thereby preventing apoptosis triggered by tumor necrosis factor- α (Pham et al., 2004). Similarly, in tobacco, ectopic expression of alfalfa ferritin enhances tolerance to ROS and the necrosis caused by viral and fungal infections (Deák et al., 1999), again supporting a defense role for Fe depletion. Although further investigation will be needed to characterize the individual proteins and pathways that cause the observed changes in Fe homeostasis during plant-pathogen interactions, our results provide a conceptual framework, linking plant and animal diseases.

Redox-active Fe as a signal in plant defense?

Identification of Fe as a mediator in plant defense responses exposes a new layer of plant defense. The data presented here have so far only been tested in monocot species and therefore cannot be applied to dicot systems with great certainty; we are, however, currently examining the role of Fe in dicot defenses using *Arabidopsis*. Despite numerous studies linking the production of ROS to defense responses, the role of ROS or changing redox conditions in plant defense is far from clear (Fobert and Despres, 2005). A hypothetical model of the status and effects of Fe during *Bgt* attack of wheat leaves is shown in Fig. 7. After pathogen attack, the plant perceives the pathogen-associated molecular pattern and initiates the targeted redistribution of redox-active Fe. Accompanying the perturbation of Fe homeostasis is the production of apoplastic H_2O_2 and activation of redox-dependent defense gene expression. The primary oxidative burst then promotes further Fe efflux and H_2O_2 production, forming a self-amplification loop. This local amplification circuit might relay to adjacent cells and even to distant (systemic) cells, and thus prolong and potentiate secondary H_2O_2 -dependent defense signaling or SAR (Levine et al., 1994; Alvarez et al., 1998). The ubiquity, mobility and reactivity of Fe make it a feasible component or cofactor of signaling in the plant defense response.

Materials and Methods

Wheat pathogen infection and cDNA library

Plant and fungal materials and handling and construction of the pathogen-induced epidermis cDNA library were performed as described (Liu et al., 2005).

Metal element analysis

The metal Fe contents were determined using a PQ II Turbo⁺ quadrupole inductively

coupled plasma mass spectrometer (ICPMS) (VG Elemental). Samples 24 hpi with *Bgt* or samples treated with 500 μM Fe^{3+} -EDTA in a time course were powdered by grinding in liquid N_2 , dried overnight at 70°C and then digested completely in 70% HNO_3 at 120°C. Before analysis, solutions were diluted by a factor of 100, and indium and bismuth were added to aliquots as internal standards for drift correction.

EPR spectroscopy

EPR experiments were performed on a Bruker EMX spectrometer equipped with an Oxford cryostat. Samples were packed into 3 mm i.d. quartz tubes that were screened for background signal. The 4.2 K EPR experiments were performed with the spectrometer frequency at 9.39 GHz, sweep width 3000 G, modulation amplitude of 1 G, power 2 mW, 100 KHz modulation frequency, gain 2×10^4 , and 12 scans at 335 seconds/scan. High resolution EPR experiments were performed at 10 K and at 50 K with the spectrometer frequency at 9.39 GHz, sweep width 40 G, modulation amplitude of 0.3 G, power 2 mW, 100 KHz modulation frequency, gain 2×10^5 , and 12 scans at 83 seconds/scan.

Histological staining and light microscopy

Staining of Fe in *Bgt*-infected epidermal cells was adapted from the method previously described (Smith et al., 1997). The H_2O_2 detection method has also been described (Thordal-Christensen et al., 1997). Double detection of Fe and H_2O_2 was performed with 3,3'-DAB (Sigma) staining first, followed by Prussian Blue staining.

In vitro assay of DAB reactions

In an attempt to differentiate between the chemistry of DAB oxidation (brown color) mediated by different substrates and the effect of DFO on these reactions, we monitored the DAB color reactions in a 96-well plate. The plate contained different combinations of reagents plus 1 mM of DAB (200 μl total per well) and was incubated at room temperature. The color was recorded by scanning the plate at different time points. DAB was added to the solution immediately after other reagents were incorporated, except assays with DFO, in which the mixtures were preincubated for 20 minutes prior to the addition of DAB. The final concentrations of the reagents were as follows: 1 mM H_2O_2 ; 0.1 U/ μl horseradish peroxidase (Sigma) (in 20 mM phosphate buffer stock, pH 6.5); 2 mM DFO; 50 μM ferric citrate.

Confocal microscopy of calcein fluorescence

Leaf epidermis 24 hpi was incubated in 1.5 mM cell-impermeable calcein (Molecular Probes) for 20 minutes to determine chelatable Fe in CWAs. Information and references relating to calcein can be found at <http://probes.invitrogen.com>. The Fe-mediated fluorescence quenching was recorded by confocal laser scanning microscopy (Petrat et al., 2001) (LSM 510; Zeiss) with excitation/emission at 488/515 nm and 1% argon laser output. After the fluorescence measurements, labile Fe was removed from calcein by adding 10 mM DFO to the sample for 30 minutes. Cell-permeable calcein-AM (Molecular Probes) was used to measure cytosolic Fe in wheat suspension cells (Clarke et al., 2000). Freshly cultured cells were washed in a Fe-free solution and placed in 2 μM calcein-AM. The dye uptake dynamics were optimized in a time course using the confocal microscope (Zeiss). The fluorescence was recorded immediately after adding 10 mM H_2O_2 to cells that had previously been incubated in 2 μM calcein-AM for 20 minutes.

Cytochalasin A and DFO treatment for cytological observations

The cut ends of primary leaves of 7-day-old wheat leaves 0.5 hpi with *Bgt* were immersed in a solution of 0.1–10 $\mu\text{g}/\text{ml}$ cyA (Sigma) for 23.5 hours before staining for Fe with Prussian Blue, or in 0.1–10 mM DFO for 6 hours before the addition of DAB for an additional 17.5 hours. To increase the contrast between conidia and plant epidermis, the DAB-stained samples were briefly stained with 0.01% aniline blue after DFO treatment.

Plant treatment with Fe and other chemicals

Cut ends of primary leaves of 7-day-old wheat seedlings were used in all the chemical treatments. The chemicals were purchased from Sigma. For Fe loading, the plants were transferred to 500 μM Fe^{3+} -EDTA, and sampled at 1, 6, 12 and 24 hours. For Fe concentration-dependent assays, the plants were transferred to solution with various concentrations of Fe^{3+} -EDTA or 500 μM EDTA. For the time-course study, the plants were treated with 500 μM Fe^{3+} -EDTA or 500 μM EDTA and collected at 1, 6, 12 and 24 hours. For the effect of reduced GSH on the Fe-induced gene expression, the plants were treated with 5 mM GSH for 3 hours followed by treatment with 500 μM Fe^{3+} -EDTA. To study the effect of DFO on defense gene expression, the plants were treated with either deionized water or 5 mM DFO for 6 hours and then sprayed with 10 mM H_2O_2 .

RNA analysis and RT-PCR

Total RNA extraction, Northern blots and tissue-specific RT-PCR were performed as described (Liu et al., 2005). The reverse primers were chosen from the 3'-UTRs whenever possible to ensure specificity. The genes used for Northern blot analyses and primer sequences for *TmFER1*, *TmNAS1*, *TmPR1a*, *TmPR1b*, *TmPR5*, *TmGLP4*

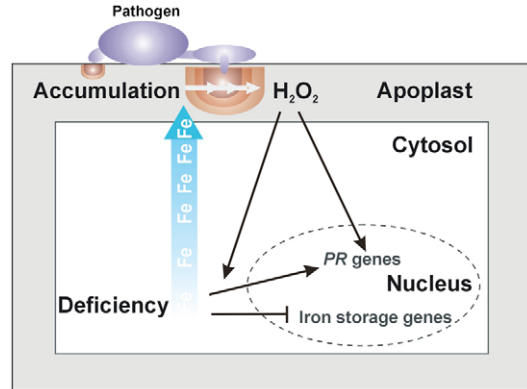


Fig. 7. The proposed role of Fe homeostasis in plant defense responses. Pathogen attack elicits the targeted Fe redistribution to the apoplast, which leads to Fe deficiency in the cytosol of attacked cells. The accumulated apoplastic Fe mediates the oxidative burst, which further stimulates Fe efflux and intracellular Fe deficiency. H_2O_2 and Fe deficiency induce expression of defense-related genes while suppressing the expression of Fe storage-related genes.

and *TmGPD1* are listed in Supplementary material Table S2. At least three biological replicates were performed for all expression analyses.

Fe-efflux measurement in wheat suspension cells

Wheat suspension cell line HY320 was maintained at room temperature with shaking at 150 rpm in MS-B5 (Sigma) liquid medium supplemented with 1.1 mg/L 2,4-dichlorophenoxyacetic acid. Freshly subcultured cells (~0.05 g fresh weight/ml) collected in Fe-free medium were treated for a time course (0.5–48 hours) with 10 mM of H_2O_2 or treated with different concentrations of H_2O_2 (1–40 mM) for a period of time. The conditions of treatment were optimized based on the above time- and concentration-dependence measurements. A G/GO approach was applied to mimic H_2O_2 -generation (Alvarez et al., 1998) with some modification. D-glucose and *Aspergillus niger* glucose oxidase (Sigma) prepared with 20 mM Na-phosphate buffer (pH 6.5) were added to cell suspensions to a final concentration of 5 mM and 5 U/ml, respectively. Vanadate (100 μM), catalase (100 U/ml) or cycloheximide (20 or 200 μM) (all from Sigma) was incorporated as required. The efflux of Fe was monitored using a spectrophotometer (DU-530; Beckman-Coulter) by measuring the absorbance of Fe^{2+} -Ferrozine complex at 562 nm after adding 5% ascorbic acid and 1 mM of Ferrozine (3-(2-pyridyl)-5,6-diphenyl-1,2,4-triazine-4', 4'-disulfonic acid) (Sigma) to the cell supernatants.

Accession numbers

The nucleotide sequences reported in this study have been submitted to the GenBank/EBI Data Bank with accession numbers *TmPR1a*, DQ167191; *TmPR1b*, DQ167192; *TmPR5*, DQ167193; *TmGLP4*, AY650052; *TmNAS1*, DQ167190; *TmFER1*, AY650054; *TmGPD1*, AY857765. Accession numbers of the array features are listed in Supplementary material Table S1.

We thank K. Wilson for critically reading the manuscript, N. Bhuiyan and X. Wu for technical support, and K. Kartha and K. Caswell for wheat suspension culture. This work was supported by grants from the National Science and Engineering Research Council of Canada (NSERC) and the Canada Foundation for Innovation to Y.W., from the Genomics and Health Initiative of NRC to G.S., and by scholarships from the Canadian Wheat Board and NSERC to D.L.G.

References

- Alford, C. E., King, T. E., Jr and Campbell, P. A. (1991). Role of transferrin, transferrin receptors, and iron in macrophage listericidal activity. *J. Exp. Med.* **174**, 459–466.
- Alvarez, M. E., Pennell, R. I., Meijer, P. J., Ishikawa, A., Dixon, R. A. and Lamb, C. (1998). Reactive oxygen intermediates mediate a systemic signal network in the establishment of plant immunity. *Cell* **92**, 773–784.
- An, Q., Huckelhoven, R., Kogel, K. H., van Bel, A. J. (2006). Multivesicular bodies participate in a cell wall-associated defence response in barley leaves attacked by the pathogenic powdery mildew fungus. *Cell. Microbiol.* **8**, 1009–1019.
- Assaad, F. E., Qiu, J.-L., Youngs, H., Ehrhardt, D., Zimmerli, L., Kalde, M., Wanner, G., Peck, S. C., Edwards, H., Ramonell, K. et al. (2004). The PEN1 syntaxin defines

- a novel cellular compartment upon fungal attack and is required for the timely assembly of papillae. *Mol. Biol. Cell* **15**, 5118-5129.
- Bolwell, G. P., Bindschedler, L. V., Blee, K. A., Butt, V. S., Davies, D. R., Gardner, S. L., Gerrish, C. and Minibayeva, F.** (2002). The apoplastic oxidative burst in response to biotic stress in plants: a three-component system. *J. Exp. Bot.* **53**, 1367-1376.
- Briat, J. F., Lobreaux, S., Grignon, N. and Vansuyt, G.** (1999). Regulation of plant ferritin synthesis: how and why. *Cell. Mol. Life Sci.* **56**, 155-166.
- Buschges, R., Hollricher, K., Panstruga, R., Simons, G., Wolter, M., Frijters, A., van Daelen, R., van der Lee, T., Diergaarde, P., Groenendijk, J. et al.** (1997). The barley *Mlo* gene: a novel control element of plant pathogen resistance. *Cell* **88**, 695-705.
- Caltagirone, A., Weiss, G. and Pantopoulos, K.** (2001). Modulation of cellular iron metabolism by hydrogen peroxide. Effects of H₂O₂ on the expression and function of iron-responsive element-containing mRNAs in B6 fibroblasts. *J. Biol. Chem.* **276**, 19738-19745.
- Choi, E. Y., Kim, E. C., Oh, H. M., Kim, S., Lee, H. J., Cho, E. Y., Yoon, K. H., Kim, E. A., Han, W. C., Choi, S. C. et al.** (2004). Iron chelator triggers inflammatory signals in human intestinal epithelial cells: involvement of p38 and extracellular signal-regulated kinase signaling pathways. *J. Immunol.* **172**, 7069-7077.
- Clarke, A., Desikan, R., Hurst, R. D., Hancock, J. T. and Neill, S. J.** (2000). NO way back: nitric oxide and programmed cell death in Arabidopsis thaliana suspension cultures. *Plant J.* **24**, 667-677.
- Clay, M. D., Jenney, F. E., Jr, Hagedoorn, P. L., George, G. N., Adams, M. W. and Johnson, M. K.** (2002). Spectroscopic studies of *Pyrococcus furiosus* superoxide reductase: implications for active-site structures and the catalytic mechanism. *J. Am. Chem. Soc.* **124**, 788-805.
- Collins, N. C., Thordal-Christensen, H., Lipka, V., Bau, S., Kombrink, E., Qiu, J. L., Huckelhoven, R., Stein, M., Freialdenhoven, A., Somerville, S. C. et al.** (2003). SNARE-protein-mediated disease resistance at the plant cell wall. *Nature* **425**, 973-977.
- Curie, C. and Briat, J. F.** (2003). Iron transport and signaling in plants. *Annu. Rev. Plant Biol.* **54**, 183-206.
- Deák, M., Horváth, G. V., Davletova, S., Török, K., Sass, L., Vass, I., Barna, B., Király, Z. and Dudits, D.** (1999). Plants ectopically expressing the iron binding protein, ferritin, are tolerant to oxidative damage and pathogens. *Nat. Biotechnol.* **17**, 192-196.
- Dellagi, A., Rigault, M., Segond, D., Roux, C., Kraepiel, Y., Cellier, F., Briat, J. F., Gaymard, F. and Expert, D.** (2005). Siderophore-mediated upregulation of Arabidopsis ferritin expression in response to *Erwinia chrysanthemi* infection. *Plant J.* **43**, 262-272.
- Expert, D.** (1999). Withholding and exchanging iron: interactions between *Erwinia* spp. and their plant hosts. *Annu. Rev. Phytopathol.* **37**, 307-334.
- Fobert, P. R. and Despres, C.** (2005). Redox control of systemic acquired resistance. *Curr. Opin. Plant Biol.* **8**, 1-5.
- Hall, J. L. and Williams, L. E.** (2003). Transition metal transporters in plants. *J. Exp. Bot.* **54**, 2601-2613.
- Hentze, M. W., Muckenthaler, M. U. and Andrews, N. C.** (2004). Balancing acts: molecular control of mammalian iron metabolism. *Cell* **117**, 285-297.
- Hiesinger, P. R., Fayyazuddin, A., Mehta, S. Q., Rosenmund, T., Schulze, K. L., Zhai, R. G., Verstreken, P., Cao, Y., Zhou, Y., Kunz, J. et al.** (2005). The v-ATPase V0 subunit a1 is required for a late step in synaptic vesicle exocytosis in *Drosophila*. *Cell* **121**, 607-620.
- Hissen, A. H. T., Wan, A. N. C., Warwas, M. L., Pinto, L. J. and Moore, M. M.** (2005). The *Aspergillus fumigatus* siderophore biosynthetic gene *sidA*, encoding L-Ornithine N5-oxygenase, is required for virulence. *Infect. Immun.* **73**, 5493-5503.
- Hückelhoven, R. and Kogel, K.-H.** (2003). Reactive oxygen intermediates in plant-microbe interactions: who is who in powdery mildew resistance? *Planta* **216**, 891-902.
- Hückelhoven, R., Fodor, J., Preis, C. and Kogel, K.-H.** (1999). Hypersensitive cell death and papilla formation in barley attacked by the powdery mildew fungus are associated with hydrogen peroxide but not with salicylic acid accumulation. *Plant Physiol.* **119**, 1251-1260.
- Keyer, K. and Imlay, J. A.** (1996). Superoxide accelerates DNA damage by elevating free-iron levels. *Proc. Natl. Acad. Sci. USA* **93**, 13635-13640.
- Kobayashi, Y., Kobayashi, I., Funaki, Y., Fujimoto, S., Takemoto, T. and Kunoh, H.** (1997). Dynamic re-organization of microfilaments and microtubules is necessary for the expression of non-host resistance in barley coleoptile cells. *Plant J.* **11**, 525-537.
- Koh, S., André, A., Edwards, H., Ehrhardt, D. and Somerville, S.** (2005). Arabidopsis thaliana subcellular responses to compatible *Erysiphe cichoracearum* infections. *Plant J.* **44**, 516-529.
- Levine, A., Tenhaken, R., Dixon, R. and Lamb, C.** (1994). H₂O₂ from the oxidative burst orchestrates the plant hypersensitive disease resistance response. *Cell* **79**, 583-593.
- Ling, H. Q., Koch, G., Baumlein, H. and Ganai, M. W.** (1999). Map-based cloning of chloronerva, a gene involved in iron uptake of higher plants encoding nicotianamine synthase. *Proc. Natl. Acad. Sci. USA* **96**, 7098-7103.
- Lipka, V., Dittgen, J., Bednarek, P., Bhat, R., Wiermer, M., Stein, M., Landtag, J., Brandt, W., Rosahl, S., Scheel, D. et al.** (2005). Pre- and postinvasion defenses both contribute to nonhost resistance in Arabidopsis. *Science* **310**, 1180-1183.
- Liu, G., Sheng, X., Greenshields, D. L., Ogieglo, A., Kaminskyj, S., Selvaraj, G. and Wei, Y.** (2005). Profiling of wheat class III peroxidase genes derived from powdery mildew-attacked epidermis reveals distinct sequence-associated expression patterns. *Mol. Plant Microbe Interact.* **18**, 730-741.
- Mathur, J. and Chua, N.-H.** (2000). Microtubule stabilization leads to growth reorientation in Arabidopsis trichomes. *Plant Cell* **12**, 465-477.
- Mittler, R., Vanderauwera, S., Gollery, M. and Van Breusegem, F.** (2004). Reactive oxygen gene network of plants. *Trends Plant Sci.* **9**, 490-498.
- Muckenthaler, M., Richter, A., Gunkel, N., Riedel, D., Polycarpou-Schwarz, M., Hentze, S., Falkenhahn, M., Stremmel, W., Ansoerge, W. and Hentze, M. W.** (2003). Relationships and distinctions in iron-regulatory networks responding to interrelated signals. *Blood* **101**, 3690-3698.
- Negishi, T., Nakanishi, H., Yazaki, J., Kishimoto, N., Fujii, F., Shimbo, K., Yamamoto, K., Sakata, K., Sasaki, T., Kikuchi, S. et al.** (2002). cDNA microarray analysis of gene expression during Fe-deficiency stress in barley suggests that polar transport of vesicles is implicated in phytosiderophore secretion in Fe-deficient barley roots. *Plant J.* **30**, 83-94.
- Nishimura, M., Stein, M., Hou, B.-H., Vogel, J., Edwards, H. and Somerville, S.** (2003). Loss of a callose synthase results in salicylic acid-dependent disease resistance. *Science* **301**, 969-972.
- Passardi, F., Penel, C. and Dunand, C.** (2004). Performing the paradoxical: how plant peroxidases modify the cell wall. *Trends Plant Sci.* **9**, 534-540.
- Petit, J. M., van Wuytswinkel, O., Briat, J. F. and Lobreaux, S.** (2001). Characterization of an iron-dependent regulatory sequence involved in the transcriptional control of *AtFer1* and *ZmFer1* plant ferritin genes by iron. *J. Biol. Chem.* **276**, 5584-5590.
- Petrat, F., de Groot, H. and Rauen, U.** (2001). Subcellular distribution of chelatable iron: a laser scanning microscopic study in isolated hepatocytes and liver endothelial cells. *Biochem. J.* **356**, 61-69.
- Pham, C. G., Bubic, C., Zazzeroni, F., Papa, S., Jones, J., Alvarez, K., Jayawardena, S., De Smaele, E., Cong, R., Beaumont, C. et al.** (2004). Ferritin heavy chain upregulation by NF- κ B inhibits TNF α -induced apoptosis by suppressing reactive oxygen species. *Cell* **119**, 529-542.
- Pich, A., Manteuffel, R., Hillmer, S., Scholz, G. and Schmidt, W.** (2001). Fe homeostasis in plant cells: does nicotianamine play multiple roles in the regulation of cytoplasmic Fe concentration? *Planta* **213**, 967-976.
- Pierre, J. L. and Fontecave, M.** (1999). Iron and activated oxygen species in biology: the basic chemistry. *BioMetals* **12**, 195-199.
- Schaible, U. E. and Kaufmann, S. H. E.** (2004). Iron and microbial infection. *Nat. Rev. Microbiol.* **2**, 946-953.
- Schrettl, M., Bignell, E., Kragl, C., Joechl, C., Rogers, T., Arst, H. N., Jr, Haynes, K. and Haas, H.** (2004). Siderophore biosynthesis but not reductive iron assimilation is essential for *Aspergillus fumigatus* virulence. *J. Exp. Med.* **200**, 1213-1219.
- Schulze-Lefert, P.** (2004). Knocking on the heaven's wall: pathogenesis of and resistance to biotrophic fungi at the cell wall. *Curr. Opin. Plant Biol.* **7**, 377-383.
- Scott-Craig, J. S., Kerby, K. B., Stein, B. D. and Somerville, S. C.** (1995). Expression of an extracellular peroxidase that is induced in barely (*Hordeum vulgare*) by the powdery mildew pathogen (*Erysiphe graminis* f. sp. hordei). *Physiol. Mol. Plant Pathol.* **47**, 407-418.
- Škalamera, D. and Heath, M. C.** (1998). Changes in the cytoskeleton accompanying infection-induced nuclear movements and the hypersensitive response in plant cells invaded by rust fungi. *Plant J.* **16**, 191-200.
- Smith, M. A., Harris, P. L. R., Sayre, L. M. and Perry, G.** (1997). Iron accumulation in Alzheimer disease is a source of redox-generated free radicals. *Proc. Natl. Acad. Sci. USA* **94**, 9866-9868.
- Stein, M., Dittgen, J., Sánchez-Rodríguez, C., Hou, B.-H., Molina, A., Schulze-Lefert, P., Lipka, V. and Somerville, S.** (2006). Arabidopsis PEN3/PDR8, an ATP binding cassette transporter, contributes to nonhost resistance to inappropriate pathogens that enter by direct penetration. *Plant Cell* **18**, 731-746.
- Takemoto, D., Jones, D. A. and Hardham, A. R.** (2003). GFP-tagging of cell components reveals the dynamics of subcellular re-organization in response to infection of Arabidopsis by oomycete pathogens. *Plant J.* **33**, 775-792.
- Thomas, F., Serratrice, G., Béguin, C., Aman, E. S., Pierre, J. L., Fontecave, M. and Lahlère, J. P.** (1999). Calcein as a fluorescent probe for ferric iron. Application to iron nutrition in plant cells. *J. Biol. Chem.* **274**, 13375-13383.
- Thordal-Christensen, H., Zhang, Z., Wei, Y. and Collinge, D. B.** (1997). Subcellular localization of H₂O₂ in plants. H₂O₂ accumulation in papillae and hypersensitive response during the barley-powdery mildew interaction. *Plant J.* **11**, 1187-1194.
- Torres, M. A., Dangel, J. L. and Jones, J. D. G.** (2002). Arabidopsis gp91^{phox} homologues *AtbbohD* and *AtbbohF* are required for accumulation of reactive oxygen intermediates in the plant defense response. *Proc. Natl. Acad. Sci. USA* **99**, 517-522.
- Torti, F. M. and Torti, S. V.** (2002). Regulation of ferritin genes and proteins. *Blood* **99**, 3505-3516.
- Walter, P. B., Knutson, M. D., Paler-Martinez, A., Lee, S., Xu, Y., Viteri, F. E. and Ames, B. N.** (2002). Iron deficiency and iron excess damage mitochondria and mitochondrial DNA in rats. *Proc. Natl. Acad. Sci. USA* **99**, 2264-2269.
- Wang, D., Weaver, N. D., Kesarwani, M. and Dong, X.** (2005). Induction of protein secretory pathway is required for systemic acquired resistance. *Science* **308**, 1036-1040.
- Watts, R. N., Hawkins, C., Ponka, P. and Richardson, D. R.** (2006). Nitrogen monoxide (NO)-mediated iron release from cells is linked to NO-induced glutathione efflux via multidrug resistance-associated protein 1. *Proc. Natl. Acad. Sci. USA* **103**, 7670-7675.
- Wei, Y., Zhang, Z., Andersen, C. H., Schmelzer, E., Gregersen, P. L., Collinge, D. B., Smedegaard-Petersen, V. and Thordal-Christensen, H.** (1998). An epidermal/papilla-specific oxalate oxidase-like protein in the defense response of barley attacked by the powdery mildew fungus. *Plant Mol. Biol.* **36**, 101-112.
- Wilson, T. J., Thomsen, K. K., Petersen, B. O., Duus, J. O. and Oliver, R. P.** (2003). Detection of 3-hydroxykynurenine in a plant pathogenic fungus. *Biochem. J.* **371**, 783-788.